Highlights

Reliability Analysis Combining Method of Moments with Control Variates

Cristóbal H. Acevedo, Xuan-Yi Zhang, Marcos A. Valdebenito, Matthias G.R. Faes

- Reliability analysis approach combining Method of Moments and Control Variates (CV).
- Unbiased estimators for the third and fourth raw moments, along with their variances.
- Efficiency of the proposed method is independent of dimensionality.
- Accurate for estimating small failure probability of weakly non-Gaussian problems.
- The method's efficiency relies on the quality of the low-fidelity model.

Reliability Analysis Combining Method of Moments with Control Variates

Cristóbal H. Acevedo[a], Xuan-Yi Zhang[b,a,*], Marcos A. Valdebenito[a], Matthias G.R. Faes[a,c]

[a] *Chair for Reliability Egineering, TU Dortmund University, , Dortmund, 44227, Leonhard-Euler-Str. 5, Germany*
[b] *National Key Laboratory of Bridge Safety and Resilience, Beijing University of Technology, , Beijing, 100124, , China*
[c] *International Joint Research Center for Engineering Reliability and Stochastic Mechanics, Tongji University, , Shanghai, 200092, , China*

Abstract

Estimating failure probabilities is a critical challenge in practice, due to high-dimensional parameter spaces and small failure probability levels. Existing sample-based methods are dimensionally robust but face efficiency challenges when estimating small failure probabilities. Approximate methods provide a balance between accuracy and computational efficiency; however, their performance is often sensitive to the dimensionality of the parameter spaces. Among existing approximate methods, Method of Moments (MoM) estimates failure probabilities by utilizing the higher-order moments of the performance function. While it provides analytical efficiency, it faces challenges in high-dimensional problems due to the difficulties in efficient moment estimation. Control Variates (CV), a variance reduction technique based on sampling, enhances moment estimation with efficiency independent of dimensionality by leveraging numerical models of different fidelities. However, it is rarely applied to the estimation of higher-order moments. This paper introduces an approach for reliability analysis that combines MoM with CV, proposing estimators for the third and fourth raw moments of the performance function based on CV. The approach achieves significant computational savings in small failure probability problems and demonstrates strong potential for high-dimensional applications. The effectiveness of the proposed approach is validated through three numerical examples, including non-Gaussian problems, computationally intensive finite element models, and nonlinear dynamic systems. The results highlight its accuracy and efficiency.

Keywords: Failure probability, Method of Moments, Control variates, High dimension, Small failure probability

---

1. Introduction

Failure probability is a key metric for assessing system reliability and risk. It is mathematically defined as a multi-dimensional integral of the joint probability density function (JPDF) of random parameters over the failure domain. In practical scenarios, failure events are typically rare, making the failure probability small and the failure domain difficult to evaluate. Furthermore, the parameter space is often high-dimensional, which increases the computational complexity of integral estimation. Achieving both efficiency and precision in estimating failure probability remains a challenging task.

There exists a diverse range of methods for estimating failure probabilities, each tailored to address specific computational and modeling challenges. One such approach is sample-based methods, which offer advantages in handling high-dimensional problems. The most straightforward method is Monte Carlo Simulation (MCS). While MCS delivers unbiased results, it is computationally demanding, requiring a large number of samples to reduce the variance of the failure probability estimator, particularly for small failure probabilities. To address this, Control Variates (CV), an effective

*E-mail: zhangxuanyi@bjut.edu.cn

variance reduction technique, has been employed for estimating small failure probabilities. However, the effectiveness of CV diminishes significantly for rare events, making it unsuitable for efficiently estimating very small failure probabilities [1, 2]. To improve the efficiency, some improved sample-based methods have been proposed such as importance sampling [3], importance sampling combined with CV [4], directional importance sampling [5, 6], and subset simulation [7, 8]. Although the efficiency has been significantly improved compared with crude MCS, efficiency issues persist in these sample-based methods when dealing with very small failure probabilities.

To overcome the difficulties associated with the calculation of small failure probabilties, approximate methods such as the First-Order Reliability Method (FORM) and Second-Order Reliability Method (SORM) have been developed [9, 10]. These methods define the failure domain using approximated LSFs, and estimate the failure probability based on the most probable points identified through optimization techniques [11]. Although approximate methods significantly improve efficiency, the approximation of LSFs can lead to inaccuracies in highly nonlinear problems or high dimensional problems [12]. As an alternative to approximate methods, surrogate models have been introduced to approximate the computationally expensive evaluations of LSFs. Examples includes Kriging models [13, 14, 15], polynomial chaos expansion [16, 17], response surface methods [18, 19], and Bayesian active learning methods [20, 21]. With efficient surrogate models applied, the computational efficiency for reliability analysis can be significantly improved. However, the construction of surrogate models introduces additional challenges, particularly in high-dimensional problems [22].

Another class of approaches assesses failure probability by computing a multi-dimensional integral of the JPDF of random parameters across the entire domain. This evaluation not only determines the failure probability but also reveals the probability distribution of the performance function. Building on the evolution mechanism of probability density in stochastic systems, the Probability Density Evolution Method (PDEM) [23] is introduced to construct the distribution function of the performance function. Based on the probability density integral equation, Direct Probability Integral Method [24] is proposed to construct the distribution function of stochastic responses of dynamic systems. Although these methods have proven effective in assessing the reliability of large structures [25], their current application is limited to problems with a small number of random variables [26]. To overcome the challenge of constructing the full distribution of the performance function, Method of Moments (MoM) is proposed to estimate the failure probability using first the three or four moments of the performance function [27, 28]. Once moments are obtained, MoM can estimate the failure probability through analytical formulas. A key task in MoM is estimating moments of the performance function, which are typically computed using dimension reduction techniques combined with point estimation method [29, 30]. However, the application of point estimation methods faces efficiency challenges in high-dimensional problems. Additionally, dimension reduction techniques may introduce inaccuracies, particularly in strongly nonlinear problems, where errors cannot be measured.

Challenges in moment estimation can be tackled using sample-based methods combined with multifidelity models. Sample-based methods are independent of problem dimensionality and provide variance estimators to assess accuracy, while multifidelity models enhance efficiency. Most multifidelity models are applied only for estimating the mean values of the performance functions, such as Multilevel Monte Carlo (MLMC) methods [31], Multifidelity Monte Carlo (MFMC) methods [32] and Control Variates (CV) [33]. Recently, an unbiased estimator of standard deviation of performance function has been proposed using CV [34, 35] with splitting techniques. These studies demonstrate the potential of CV for improving the estimation of statistical moments, with reduced variance and computational costs. However, to the best of authors' best knowledge, there are no estimators provided for higher-order moments of the performance function based on CV.

This paper introduces a novel reliability analysis approach that synergistically combines MoM with CV. To enable this integration, the estimators for the third and fourth moments are proposed, marking the first application of such estimators within the CV framework (to the best knowledge of the authors). By leveraging the explicit failure probability model based on moments of the performance function provided by MoM, and the efficient moment estimation enabled by CV, the proposed approach addresses the inherent limitations of each method. Specifically, it overcomes the infeasibility of high-dimensional moment estimation in MoM and the challenges in directly evaluating failure probability using CV. The result is an approach that not only achieves significant computational savings for estimating small failure probability but also demonstrates strong potential for effectively handling high-dimensional problems. The structure of the paper is as follows: Section 2 reviews the fundamentals of MoM. Section 3 details the CV and its application for variance reduction, with the estimators for third and fourth order moments proposed. Procedures of the proposed method are discussed in Section 4. The Section 5 demonstrates the efficiency and accuracy of the proposed method through three numerical examples. Finally, Section 6 concludes the paper.

2. Failure probability based on Method of Moments

2.1. Problem statement

A fundamental problem in reliability analysis is computing the failure probability, denoted as P_F, which is the likelihood of a failure event of interest and can be formulated as follows:

$$P_F = \mathrm{Prob}[G(\mathbf{X}) \leq 0], \tag{1}$$

where $\mathrm{Prob}[\cdot]$ is the probability operator; $G(\mathbf{X})$ is the performance function associated with the failure event of interest, where $G(\mathbf{X}) \leq 0$ indicates the occurrence of failure, and $G(\mathbf{X}) > 0$ implies safety; and $\mathbf{X} = (X_1, \cdots, X_n)^T$ is a n dimensional vector of input random variables, with the ith random variable denoted by X_i. Denote the JPDF of $\mathbf{X}$ as $f_{\mathbf{X}}(\mathbf{x})$, P_F can be computed by a multifold probability integral over the failure domain as follows:

$$P_F = \int_{G(\mathbf{X})\leq 0} f_{\mathbf{X}}(\mathbf{x}) d\mathbf{x}. \tag{2}$$

In certain specific cases, such as when $G(\mathbf{X})$ is a weighted summation of independent random variables, the values of $\mathbf{X}$ that correspond to the failure domain can be explicitly determined. However, in practical engineering applications, $G(\mathbf{X})$ is often complex and may even involve finite element models (FEMs), making the estimation of the failure probability challenging or even infeasible.

2.2. Method of Moments

To address the difficulty of computing the integral over the failure domain, MoM [28] has been developed. As illustrated in Fig. 1, the core concept of MoM is to treat $G(\mathbf{X})$ as a random variable $Z = G(\mathbf{X})$, which enables the reformulation of the failure probability P_F as follows:

$$P_F = F_Z(0), \tag{3}$$

where $F_Z(\cdot)$ is the CDF of Z. The distribution of Z is generally unknown, and $F_Z(0)$ is alternatively approximated based on moments of Z alternatively. Since the first four standard central moments, i.e., the mean μ_{Z_1}, standard deviation μ_{Z_2}, skewness μ_{Z_3} and kurtosis μ_{Z_4}, contain the majority statistical information about the distribution, they are applied to approximate the distribution of Z.

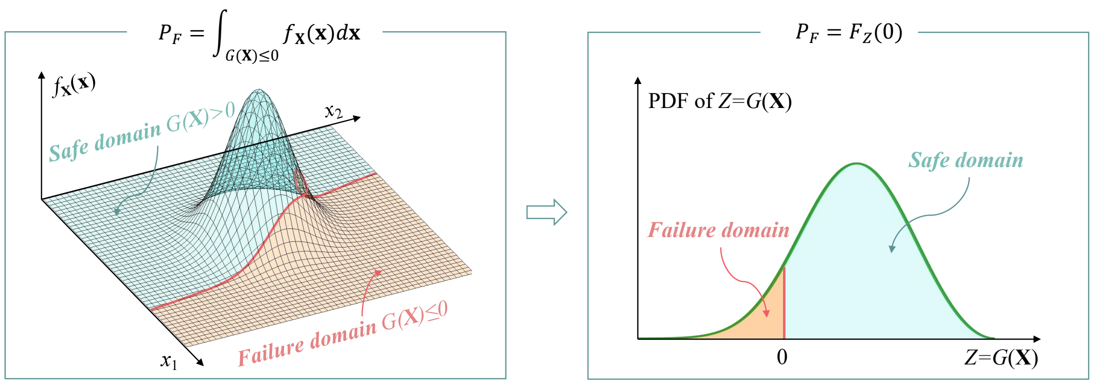

Figure 1: Schematic representation of the method of moments

To derive an explicit expression while ensuring a high level of accuracy, the cubic normal distribution [36] is applied in this study, and then $F_Z(0)$ is then computed as follows:

$$F_Z(0) \cong \Phi(\beta_{4M}), \tag{4}$$

where β_{4M} is the fourth moment reliability index, which is obtained by equivalently transforming Z=0 into Gaussian space based on the first four moments of Z and is formulated as follows [37]:

$$\beta_{4M} = \sqrt[3]{\Delta + q} - \sqrt[3]{\Delta - q} + \frac{a_3}{3a_4}, \tag{5}$$

$$\Delta = \sqrt{q^2 + p^3}, \tag{6}$$

$$p = \frac{3a_2a_4 - a_3^2}{9a_4^2}, \quad q = \frac{a_3^3}{27a_4^3} - \frac{a_2a_3}{6a_4^2} - \frac{a_3 - \beta_{2M}/a_1}{2a_4}, \quad \beta_{2M} = \frac{\mu_{Z_1}}{\mu_{Z_2}}, \tag{7}$$

where β_{2M} is the second moment reliability index; and a_2, a_3, and a_4 are the parameters calculated based on μ_{Z_3} and μ_{Z_4} as follows [38]:

$$a_2 = 1 - 3a_4, \quad a_3 = \frac{5 + (35 - \mu_{Z_3}^2)a_4^2}{9a_0 + 30 - 0.8\mu_{Z_3}^2}\mu_{Z_3}, \quad a_4 = \frac{2a_0}{2a_0 + 46(1 - 1/\mu_{Z_4}^2) - \mu_{Z_3}^2}, \tag{8}$$

$$a_0 = \frac{\sqrt{3\mu_{Z_4} - 4\mu_{Z_3}^2 - 5} - 2}{1 - (3\mu_{Z_3}^2 + 1)/\mu_{Z_4}^2}, \quad a_1 = \frac{1}{\sqrt{1 + 2a_3^2 + 6a_4^2}}. \tag{9}$$

Please note that Eqs. (5)-(7) are valid within a specific range of applicability. If the combination of μ_{Z_3} and μ_{Z_4} falls outside this range, a complete expression for β_{4M} is required [37] (for details, see Appendix A). The mean μ_{Z_1}, standard deviation μ_{Z_2}, skewness μ_{Z_3} and kurtosis μ_{Z_4} of the performance function are theoretically defined as follows:

$$\mu_{Z_1} = E_{Z_1}, \tag{10}$$

$$\mu_{Z_2} = \sqrt{E_{Z_2} - E_{Z_1}^2}, \tag{11}$$

$$\mu_{Z_3} = \frac{1}{\mu_{Z_2}^3}\left(E_{Z_3} - 3E_{Z_1}E_{Z_2} + 2E_{Z_1}^3\right), \tag{12}$$

$$\mu_{Z_4} = \frac{1}{\mu_{Z_2}^4}\left(E_{Z_4} - 4E_{Z_1}E_{Z_3} + 6E_{Z_1}^2 E_{Z_2} - 3E_{Z1}^4\right), \tag{13}$$

where E_{Z_i} is the ith raw moment, which is defined as follows:

$$E_{Z_i} = \mathbb{E}\left\{[G(\mathbf{X})]^i\right\} = \int_{\Omega_{\mathbf{X}}} [G(\mathbf{x})]^i f_{\mathbf{X}}(\mathbf{x}) d\mathbf{x}, \tag{14}$$

where $\mathbb{E}\{\cdot\}$ denotes the expectation of the argument; $\Omega_{\mathbf{x}}$ is the domain of all possible values of $\mathbf{X}$. Based on Eqs. (3)-(14), MoM computes the failure probability by integrating over the entire domain rather than the failure domain. This method overcomes the difficulty of defining the values of $\mathbf{X}$ corresponding to the failure domain and thus makes the problem tractable.

2.3. Challenge in Method of Moments

One of the key tasks in MoM is estimating raw moments of the performance function as given in Eq. (14). Since $G(\mathbf{X})$ is generally complicated, directly computing these moments from Eq. (14) is typically not feasible, and numerical methods are employed as an alternative. A basic approach is to convert the integral into a summation. However, as $\mathbf{X}$ is often high-dimensional, this computation can be time-consuming. To improve efficiency, various dimensional reduction methods have been proposed [29, 30, 39]. Despite these efforts, the number of evaluations still increases with the dimension of $\mathbf{X}$, making it impractical for high-dimensional problems. Furthermore, since moments are estimated approximately, the accuracy level of these estimates should be provided. However, there is no error estimator provided for dimensional reduction methods, leaving the accuracy of the computed failure probability uncertain.

Alternatively, MCS can be applied for moment estimation, with the estimator and corresponding variance obtained as follows:

$$\widehat{E}_{Z_i}^{\mathrm{MCS}}(\hat{\mathbf{x}}_n) = H(G^i, \hat{\mathbf{x}}_n) = \frac{1}{n}\sum_{j=1}^{n}\left[G\left(\hat{\mathbf{x}}_n^{(j)}\right)\right]^i, \tag{15}$$

$$\mathbb{V}\left[\widehat{E}_{Z_i}^{\mathrm{MCS}}(\hat{\mathbf{x}}_n)\right] = \mathbb{V}\left[H(G^i, \hat{\mathbf{x}}_n)\right] = \frac{1}{n(n-1)}\left\{\sum_{j=1}^{n}\left[G\left(\hat{\mathbf{x}}_n^{(j)}\right)\right]^{2i} - \frac{1}{n}\left[H(G^i, \hat{\mathbf{x}}_n)\right]^2\right\}, \tag{16}$$

where $\widehat{E}_{Z_i}^{\mathrm{MCS}}(\hat{\mathbf{x}}_n)$ is the estimator of ith raw moment in crude MCS based on samples $\hat{\mathbf{x}}_n$; $H(G^i, \hat{\mathbf{x}}_n)$ denotes the estimator of the ith raw moment of $G(\mathbf{X})$, based on n samples grouped in $\hat{\mathbf{x}}_n$; the matrices $\hat{\mathbf{x}}_n = \begin{bmatrix}\hat{\mathbf{x}}_n^{(1)} & \hat{\mathbf{x}}_n^{(2)} & \cdots & \hat{\mathbf{x}}_n^{(n)}\end{bmatrix}$ represents the sets of input samples used for the estimation; $\hat{\mathbf{x}}_n^{(j)}$ is the jth sample in $\hat{\mathbf{x}}_n$; n is the sample size; and $\mathbb{V}[\cdot]$ is a variance estimator. The Coefficient of Variation (CoV) of the MCS-based estimator $\widehat{E}_{Z_i}^{\mathrm{MCS}}(\hat{\mathbf{x}}_n)$ can then be estimated as follows:

$$\mathrm{CoV}\left[\widehat{E}_{Z_i}^{\mathrm{MCS}}(\hat{\mathbf{x}}_n)\right] = \frac{\sqrt{\mathbb{V}\left[\widehat{E}_{Z_i}^{\mathrm{MCS}}(\hat{\mathbf{x}}_n)\right]}}{\mathbb{E}\left[\widehat{E}_{Z_i}^{\mathrm{MCS}}(\hat{\mathbf{x}}_n)\right]}. \tag{17}$$

It can be seen from Eqs. (15)-(17) that, narrowing down the variances of MCS estimator requires a large number of samples, which is generally time-consuming. Nevertheless, keeping the coefficient of variation in Eq. (17) sufficiently low is highly desirable, as this in turn leads to a sufficiently accurate estimation of failure probabilities with MoM.

3. Moment estimation using the Control Variates technique

3.1. Basic theory of the Control Variates technique

To reduce the variance of the estimated moments, CV is introduced. Without loss of accuracy, $[G(\mathbf{X})]^i$ can be equivalently expressed as follows [40]:

$$[G(\mathbf{X})]^i = \left\{[G(\mathbf{X})]^i - \rho[L(\mathbf{X})]^i\right\} + \rho[L(\mathbf{X})]^i, \tag{18}$$

where $L(\mathbf{X})$ denotes the low-fidelity (LF) model, which produces approximate responses at a faster rate by sacrificing some accuracy; and ρ is a control parameter. Note that, in existing studies, only the cases with $i = 1$ or 2 are considered, while the higher-order raw moments are investigated for the first time here (to the authors' best knowledge). For clarity, $G(\mathbf{X})$ referenced below is referred to as the high-fidelity (HF) model.

By substituting Eq. (18) into (14), the ith raw moment of $G(\mathbf{X})$ can be reformulated as follows:

$$E_{Z_i} = \int_{\Omega_{\mathbf{X}}} \left\{[G(\mathbf{x})]^i - \rho[L(\mathbf{x})]^i\right\} f_{\mathbf{X}}(\mathbf{x})d\mathbf{x} + \rho \int_{\Omega_{\mathbf{X}}} [L(\mathbf{x})]^i f_{\mathbf{X}}(\mathbf{x})d\mathbf{x}. \tag{19}$$

Based on Eq. (19), E_{Z_i} can be estimated based on two sets of samples as follows:

$$\widehat{E}_{Z_i}(\hat{\mathbf{x}}_n, \hat{\mathbf{x}}_m) = H(G^i, \hat{\mathbf{x}}_n) - \rho\left[H(L^i, \hat{\mathbf{x}}_n) - H(L^i, \hat{\mathbf{x}}_m)\right], \tag{20}$$

where $H(L^i, \hat{\mathbf{x}}_n)$ and $H(L^i, \hat{\mathbf{x}}_m)$ denote the estimators of the ith raw moment of the LF model based on n samples grouped in $\hat{\mathbf{x}}_n$ and m samples grouped in $\hat{\mathbf{x}}_m$, respectively. The variance of $\widehat{E}_{Z_i}(\hat{\mathbf{x}}_n, \hat{\mathbf{x}}_m)$ is then computed as follows:

$$\begin{aligned}\mathbb{V}\left[\widehat{E}_{Z_i}(\hat{\mathbf{x}}_n, \hat{\mathbf{x}}_m)\right] =& \mathbb{V}[H(G^i, \hat{\mathbf{x}}_n)] + \rho^2\left\{\mathbb{V}[H(L^i, \hat{\mathbf{x}}_n)] + \mathbb{V}\left[H(L^i, \hat{\mathbf{x}}_m)\right]\right\} \\ &- 2\rho\mathbb{C}\left[H(G^i, \hat{\mathbf{x}}_n), H(L^i, \hat{\mathbf{x}}_n)\right]\end{aligned}, \tag{21}$$

where $\mathbb{C}\left[H(G^i, \hat{\mathbf{x}}_n), H(L^i, \hat{\mathbf{x}}_n)\right]$ is the covariance between ith order power of the outputs from the HF and LF models, evaluated using n shared samples $\hat{\mathbf{x}}_n$, which can be computed as follows:

$$\mathbb{C}\left[H(G^i, \hat{\mathbf{x}}_n), H(L^i, \hat{\mathbf{x}}_n)\right] = \frac{1}{n(n-1)}\left\{\sum_{j=1}^{n}\left[G\left(\hat{\mathbf{x}}_n^{(j)}\right)L\left(\hat{\mathbf{x}}_n^{(j)}\right)\right]^i - \frac{1}{n}H(G^i, \hat{\mathbf{x}}_n)H(L^i, \hat{\mathbf{x}}_n)\right\}, \tag{22}$$

The purpose of CV is to minimize the variance given in Eq. (21), and thus an optimal control parameter $\rho_{\text{opt}}(i, \hat{\mathbf{x}}_n, \hat{\mathbf{x}}_m)$ can be determined, which is computed as follows [40, 32]:

$$\rho_{\text{opt}}(i, \hat{\mathbf{x}}_n, \hat{\mathbf{x}}_m) = \frac{\mathbb{C}\left[H(G^i, \hat{\mathbf{x}}_n), H(L^i, \hat{\mathbf{x}}_n)\right]}{\mathbb{V}[H(L^i, \hat{\mathbf{x}}_n)] + \mathbb{V}\left[H(L^i, \hat{\mathbf{x}}_m)\right]}. \tag{23}$$

Substitution of Eq. (23) into Eqs. (20) and (21) yields the construction of the estimator for ith raw moment of $G(\mathbf{X})$ in CV, denoted as $\widehat{E}^{\text{CV}}_{Z_i}(\hat{\mathbf{x}}_n, \hat{\mathbf{x}}_m)$. $\widehat{E}^{\text{CV}}_{Z_i}(\hat{\mathbf{x}}_n, \hat{\mathbf{x}}_m)$ and corresponding variance can be reformulated as follows [40, 32]:

$$\widehat{E}^{\text{CV}}_{Z_i}(\hat{\mathbf{x}}_n, \hat{\mathbf{x}}_m) = H(G^i, \hat{\mathbf{x}}_n) - \rho_{\text{opt}}(i, \hat{\mathbf{x}}_n, \hat{\mathbf{x}}_m)\left[H(L^i, \hat{\mathbf{x}}_n) - H(L^i, \hat{\mathbf{x}}_m)\right], \tag{24}$$

$$\mathbb{V}\left[\widehat{E}_{Z_i}^{\text{CV}}(\hat{\mathbf{x}}_n,\hat{\mathbf{x}}_m)\right]=\mathbb{V}\left[H(G^i,\hat{\mathbf{x}}_n)\right]-\frac{\left\{\mathbb{C}\left[H(G^i,\hat{\mathbf{x}}_n),H(L^i,\hat{\mathbf{x}}_n)\right]\right\}^2}{\mathbb{V}[H(L^i,\hat{\mathbf{x}}_n)]+\mathbb{V}\left[H(L^i,\hat{\mathbf{x}}_m)\right]}. \tag{25}$$

A comparison between Eqs. (16) and (25) shows that the variance of $\widehat{E}_{Z_i}^{\text{CV}}(\hat{\mathbf{x}}_n,\hat{\mathbf{x}}_m)$ is smaller than that of $\widehat{E}_{Z_i}^{\text{MCS}}(\hat{\mathbf{x}}_n)$, demonstrating the potential of using CV to achieve variance reduction. Furthermore, $\mathbb{V}\left[\widehat{E}_{Z_i}^{\text{CV}}(\hat{\mathbf{x}}_n,\hat{\mathbf{x}}_m)\right]$ decreases as the variances of $H(G^i,\hat{\mathbf{x}}_n)$, $H(L^i,\hat{\mathbf{x}}_n)$ and $H(L^i,\hat{\mathbf{x}}_m)$ decrease, while it decreases with a higher $\mathbb{C}\left[H(G^i,\hat{\mathbf{x}}_n),H(L^i,\hat{\mathbf{x}}_n)\right]$. To achieve variance reduction with fewer HF model evaluations, it is essential to minimize $\mathbb{V}[H(L^i,\hat{\mathbf{x}}_m)]$ while maximizing $\mathbb{C}\left[H(G^i,\hat{\mathbf{x}}_n),H(L^i,\hat{\mathbf{x}}_n)\right]$. Minimizing $\mathbb{V}[H(L^i,\hat{\mathbf{x}}_m)]$ requires a sufficiently large size of $\hat{\mathbf{x}}_m$, which underscores the importance of ensuring that the computational cost of evaluating the LF model remains as low as possible. Note that $\mathbb{C}\left[H(G^i,\hat{\mathbf{x}}_n),H(L^i,\hat{\mathbf{x}}_m)\right]$ quantifies the linear relationship between the HF and LF models. Therefore, a strong linear correlation between these two models is a key condition for achieving substantial variance reduction.

3.2. Unbiased estimation of raw moments using the splitting technique

To ensure there is no difference between the expectation of the estimator and the true value, the bias in the estimator of $\widehat{E}_{Z_i}^{\text{CV}}(\hat{\mathbf{x}}_n,\hat{\mathbf{x}}_m)$ should be examined. Based on Eq. (24), the bias of the estimator is quantified as follows [41]:

$$\begin{aligned}\text{Bias}\left[\widehat{E}_{Z_i}^{\text{CV}}(\hat{\mathbf{x}}_n,\hat{\mathbf{x}}_m)\right]=&\mathbb{E}\left\{\widehat{E}_{Z_i}^{\text{CV}}(\hat{\mathbf{x}}_n,\hat{\mathbf{x}}_m)-\tilde{H}(G^i)\right\}\\=&\mathbb{C}\left[\rho_{\text{opt}}(i,\hat{\mathbf{x}}_n,\hat{\mathbf{x}}_m),H(L^i,\hat{\mathbf{x}}_m)-H(L^i,\hat{\mathbf{x}}_n)\right],\end{aligned} \tag{26}$$

where $\tilde{H}(G^i)$ is the true value of the ith raw moment of the HF model. Based on Eq. (26), the bias in the estimator is given by the covariance between $\rho_{\text{opt}}(i,\hat{\mathbf{x}}_n,\hat{\mathbf{x}}_m)$ and $H(L^i,\hat{\mathbf{x}}_m)-H(L^i,\hat{\mathbf{x}}_n)$, which arises from the correlation between these two estimators when derived from the same set of samples.

To eliminate the bias while maintaining efficiency, a splitting technique has been proposed [35, 41]. This method divides the available samples into independent groups and uses separate groups to estimate the optimum control parameter and the statistics associated with the HF and LF models. This ensures the estimated values remain uncorrelated, resulting in zero bias. Generally, the available samples can be evenly divided into three groups, and the estimator of the raw moments using the splitting technique is given by [35]:

$$\widehat{E}_{Z_i}^{\text{CV-S}}(\hat{\mathbf{x}}_n,\hat{\mathbf{x}}_m)=\frac{1}{3}\sum_{j=1}^{3}\widehat{E}_{Z_i}^{j}(\hat{\mathbf{x}}_{j,n^*},\hat{\mathbf{x}}_{j,m^*},\hat{\mathbf{x}}_{\tau(j),n^*},\hat{\mathbf{x}}_{\tau(j),m^*}), \tag{27}$$

$$\begin{aligned}\widehat{E}_{Z_i}^{j}(\hat{\mathbf{x}}_{j,n^*},\hat{\mathbf{x}}_{j,m^*},\hat{\mathbf{x}}_{\tau(j),n^*},\hat{\mathbf{x}}_{\tau(j),m^*})=&H(G^i,\hat{\mathbf{x}}_{j,n^*})\\&-\rho_{\text{opt}}(i,\hat{\mathbf{x}}_{\tau(j),n^*},\hat{\mathbf{x}}_{\tau(j),m^*})\left[H(L^i,\hat{\mathbf{x}}_{j,n^*})-H(L^i,\hat{\mathbf{x}}_{j,m^*})\right],\end{aligned} \tag{28}$$

where $\widehat{E}_{Z_i}^{\text{CV-S}}(\hat{\mathbf{x}}_n,\hat{\mathbf{x}}_m)$ is the splitting-based estimator of the ith raw moment of the HF model; $\hat{\mathbf{x}}_{j,n^*}$ and $\hat{\mathbf{x}}_{j,m^*}$ denote the samples for the jth group; $n^*=n/3$ and $m^*=m/3$ are the numbers of samples per group; $\hat{\mathbf{x}}_{\tau(j),n^*}$ and $\hat{\mathbf{x}}_{\tau(j),m^*}$ denote the samples for the $\tau(j)$th group; and $\tau(j)=(j \bmod 3)+1$ is an index cycles through the values $1,2,3$.

Based on Eq. (27), the variance of $\widehat{E}_{Z_i}^{\text{CV-S}}(\hat{\mathbf{x}}_n,\hat{\mathbf{x}}_m)$ is given by:

$$\mathbb{V}\left[\widehat{E}_{Z_i}^{\text{CV-S}}(\hat{\mathbf{x}}_n,\hat{\mathbf{x}}_m)\right]=\frac{1}{3^2}\sum_{j=1}^{3}\mathbb{V}\left[\widehat{E}_{Z_i}^{j}(\hat{\mathbf{x}}_{j,n^*},\hat{\mathbf{x}}_{j,m^*},\hat{\mathbf{x}}_{\tau(j),n^*},\hat{\mathbf{x}}_{\tau(j),m^*})\right]. \tag{29}$$

The CoV of the splitting-based estimator $\widehat{E}_{Z_i}^{\text{CV-S}}$ can be expressed as follows:

$$\text{CoV}\left[\widehat{E}_{Z_i}^{\text{CV-S}}\right] = \frac{\sqrt{\mathbb{V}\left[\widehat{E}_{Z_i}^{\text{CV-S}}(\hat{\mathbf{x}}_n, \hat{\mathbf{x}}_m)\right]}}{\mathbb{E}\left[\widehat{E}_{Z_i}^{\text{CV-S}}(\hat{\mathbf{x}}_n, \hat{\mathbf{x}}_m)\right]}. \tag{30}$$

3.3. Challenges in applying Control Variates for failure probability estimation

While CV is an effective variance reduction technique for moment estimation, its application to estimating small failure probabilities encounters significant challenges, primarily due to the characteristics of rare event scenarios.

One major challenge is the low correlation in extreme events. As discussed earlier, the effectiveness of the CV method depends heavily on the correlation between HF and LF models. However, in extreme event scenarios, this correlation often diminishes significantly [1], greatly reducing the efficiency of CV. Another limitation arises from the limited contribution of samples in rare event scenarios. Small failure probabilities are typically concentrated in narrow regions of the parameter space, meaning that most samples drawn from the input distribution contribute little to the estimation process, leading to significant sampling inefficiency.

To address these challenges, combining methods has emerged as a promising strategy. By leveraging the focused sampling properties of Importance Sampling (IS), CV has been integrated with IS to achieve more efficient estimation of small failure probabilities [4]. While this combination enhances efficiency, it introduces the curse of dimensionality. Specifically, identifying suitable sampling densities for IS becomes increasingly difficult as dimensionality grows [42], making the combination of IS and CV inherently challenging for high-dimensional problems.

4. Reliability analysis using Method of Moments combining Control Variates

In the proposed method, the failure probability is computed directly based on the moments of performance function, while moment estimation is performed using CV combing with splitting technique. Detailed procedure is discussed as follows:

(1) **Moment estimation of performance function**

- **Construct low-fidelity model**. To enhance variance reduction, LF model should posses strong linear correlation with the HF model, i.e., the original model. The LF model can be constructed using simpler numerical techniques, such as finite difference methods instead of finite element methods, larger time steps, or coarser meshes.
- **Samples generation**. Generate $\hat{\mathbf{x}}_n$ and $\hat{\mathbf{x}}_m$. Compute the outputs of HF and LF models based on $\hat{\mathbf{x}}_n$ and $\hat{\mathbf{x}}_m$.
- **Raw moment estimation**. Divide the samples evenly into three groups. Compute $\widehat{E}_{Z_i}^{\text{CV-S}}(\hat{\mathbf{x}}_n, \hat{\mathbf{x}}_m)$ using Eqs. (23) and (27)-(28). Then, evaluate the CoV of $\widehat{E}_{Z_i}^{\text{CV-S}}(\hat{\mathbf{x}}_n, \hat{\mathbf{x}}_m)$ with the aid of Eqs. (25), and (29)-(30). If the obtained CoV meets the target requirement, proceed to the next step. Otherwise, adjust the sample size or modify the LF model as needed. Modifications can be guided by the values of $\mathbb{V}[H(L^i, \hat{\mathbf{x}}_{j,m^*})]$ and $\mathbb{C}\left[H(G^i, \hat{\mathbf{x}}_{j,n^*}), H(L^i, \hat{\mathbf{x}}_{j,n^*})\right]$.
  - If $\mathbb{V}[H(L^i, \hat{\mathbf{x}}_{j,m^*})]$ is relatively large, m should be increased.
  - If $\mathbb{C}\left[H(G^i, \hat{\mathbf{x}}_{j,n^*}), H(L^i, \hat{\mathbf{x}}_{j,n^*})\right]$ is small, modify the LF model to improve the linear correlation between the LF and HF models.

- **Standard central moment estimation**. With the raw moment of performance function estimated, the mean, standard deviation, skewness and kurtosis can be directly computed based on Eqs. (10)-(13).

(2) **Failure probability estimation**. The failure probability can be computed based on the standard central moments of the performance function, using explicit formulas given in Eqs. (3)-(9).

The application of CV ensures the unbiased moment estimation of the performance function using a reduced number of samples, while MoM provides efficient formula for computing failure probability based on the estimated moments. With the CoV in estimated moments provided, the reliable level of estimated failure probability can be anticipated, which is important for practical engineering.

5. Examples

To evaluate the application of the proposed method, three examples are presented in this section. The first example involves a univariate polynomial with an analytical solution for moments of the performance function and the failure probability. This example demonstrates the detailed procedure of the proposed method and explores the effects of non-Gaussianity, nonlinearity, and the failure probability level on its performance. The second example considers a seepage problem beneath a dam, incorporating a refined FEM. This example illustrates the application of the proposed method to a complex practical problem and explores the impact of LF model quality on its performance. The third example focuses on a Duffing oscillator, which is nonlinear, non-Gaussian, and high-dimensional. This example assesses the capability of the proposed method to handle computationally intensive, high-dimensional reliability problems.

5.1. Example 1: A univariate polynomial

The first example investigates an analytical problem with the performance function defined as follows:

$$G(X) = k_1 X^3 + k_2 X^2 + k_3 X + k_4, \tag{31}$$

where k_i (i =1,..,4) are polynomial coefficients and X is a random variable.

5.1.1. Detailed procedure of the proposed method

To illustrate the detailed procedure of the proposed method, the case when $k_1 = 1.0$, $k_2 = -6.0$, $k_3 = 18$, $k_4 = -8.0$ is considered, with X following a Gamma distribution with mean value $\mu_{X_1} = 1.0$ and CoV set to be 0.2. As an univariate polynomial, there are analytical solutions to the mean, standard deviation, skewness and kurtosis of the performance function, denoted by a vector $\boldsymbol{\mu}_Z = (\mu_{Z_1}, \mu_{Z_2}, \mu_{Z_3}, \mu_{Z_4})$, and failure probability, which are $\boldsymbol{\mu}_Z = (4.8832, 1.7852, 0.0188, 2.9354)$, and $P_F = 2.5271 \times 10^{-3}$, respectively (details can be found in Appendix B).

To apply the proposed method, the first step is to construct a LF model corresponding to the original performance function (HF model). In this example, a second-order Taylor expansion around μ_{X_1} is used as the LF model, defined as follows:

$$L(X) = G(\mu_{X_1}) + d_1(\mu_{X_1})(X - \mu_{X_1}) + d_2(\mu_{X_1})(X - \mu_{X_1})^2/2, \tag{32}$$

where $d_i(\mu_{X_1})$ (i=1, 2) is the ith order derivative of $G(X)$ around μ_{X_1}. The second step is to generate samples of X, i.e., $\hat{\mathbf{x}}_n$ and $\hat{\mathbf{x}}_m$, and the corresponding responses computed from the HF and LF models. To obtain a reliable evaluation of the raw moments of the performance function,

n=12,000 and $m = 3 \times 10^6$ are used in this example. The corresponding raw moments obtained are (4.8825, 27.0248, 163.15219, 1055.4837), with CoVs of (0.0215%, 0.0414%, 0.0665%, 0.1020%). Based on Eqs. (10)-(13), $\boldsymbol{\mu}_Z$ can be obtained as (4.8825, 1.7848, 0.0166, 2.9240). Substitution of $\boldsymbol{\mu}_Z$ into Eqs. (3)-(9) leads to the result of the failure probability as 2.5632×10^{-3}. Comparison between the failure probability obtained from the proposed method with the exact value shows that, the relative error is around 1.4273%. This demonstrates the accuracy of the proposed method for this case.

5.1.2. *Influence of the inputs*

To investigate the impact of the input statistical model on the performance of the proposed method, various statistical models for X are considered, including Normal, Lognormal, Gamma, Weibull and Gumbel distributions, with CoV set to be 0.1, 0.2, 0.3, 0.4, and 0.5. The variations in failure probabilities obtained through both the analytical solution and the proposed method are compared in Figs. 2a-2e.

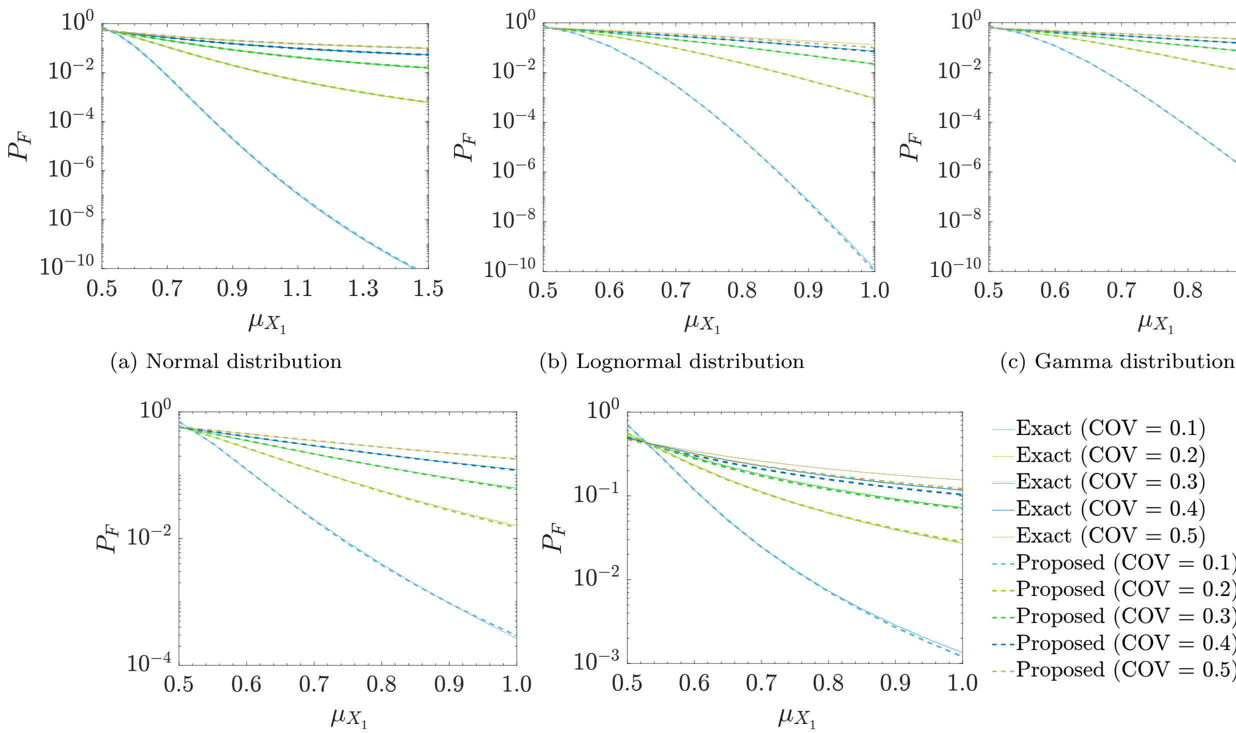

(a) Normal distribution (b) Lognormal distribution (c) Gamma distribution

(d) Weibull distribution (e) Gumbel distribution

Figure 2: Change of failure probability with mean value of X

It can be observed that when X follows Normal, Gamma, or Weibull distributions, the proposed method accurately estimates failure probabilities, which are consistent with the exact values across all considered CoVs. This demonstrates the flexibility and adaptability of the proposed method across different statistical models of the input. When X follows Lognormal or Gumbel distributions, the proposed method yields failure probabilities that closely match the exact values for smaller CoVs (less than 0.4). However, for larger CoVs, slight discrepancies arise between the results of the proposed method and the exact values. This is attributed to the increased error in MoM for strongly non-Gaussian problems.

5.1.3. Influence of the performance function

In practical engineering, the performance function defines the failure events and the relationship between the inputs and outputs. Thus, its shape will influence the performance of the proposed method. To examine the influence of the performance function, different values of k_2, k_3, and k_4 are considered with $k_1 = 1.0$, and the variations of failure probabilities obtained analytically and from the proposed method are compared in Figs. 3a-3e.

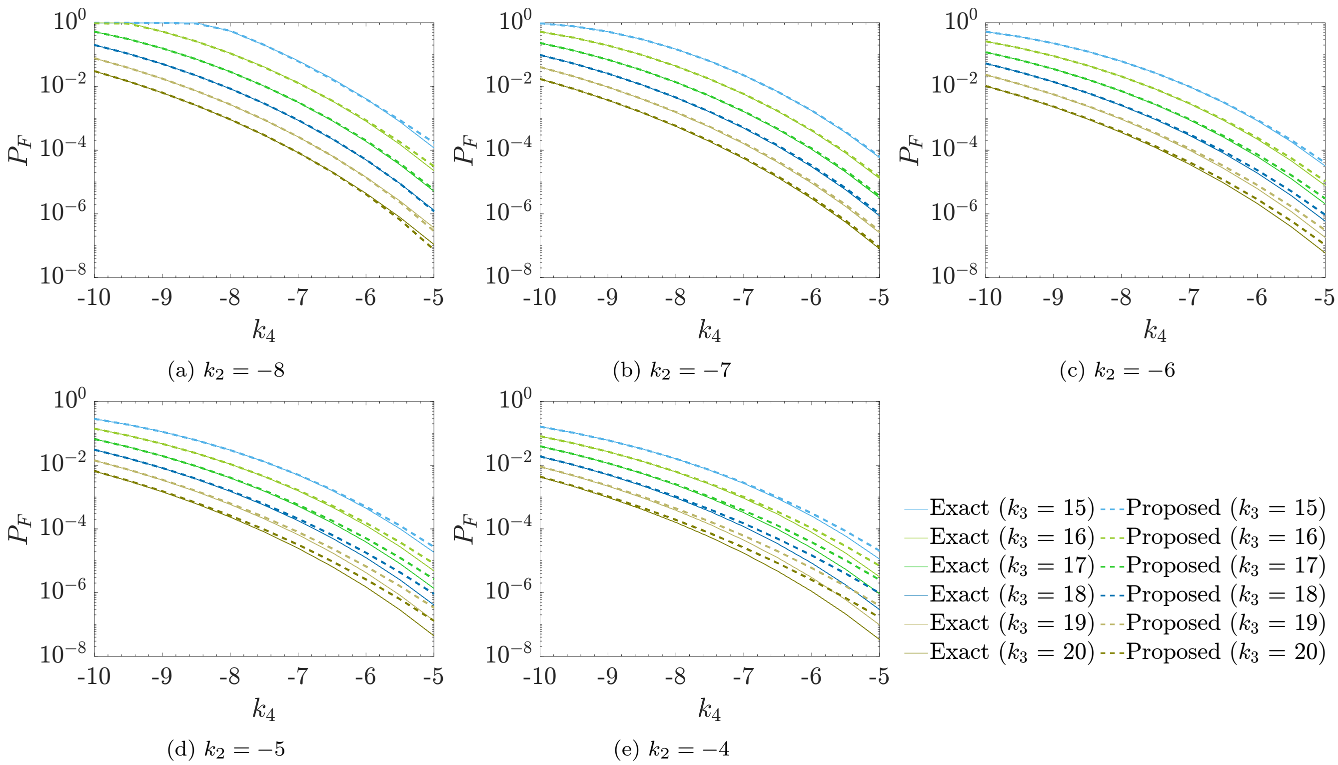

Figure 3: Change of failure probability with k_4

It can be found that:

(1) When $k_2 = -7$, the failure probability computed using the proposed method closely aligns with the reference results across all considered failure probability levels, with a minimum of approximately 10^{-8}. This is because, in this case, the performance function exhibits weak non-Gaussianity, allowing MoM to provide precise evaluations of the failure probability.

(2) When the value of k_2 deviates from -7, the difference between the failure probabilities obtained from the analytical and the proposed method becomes significant for smaller failure probabilities. For $k_2 = -8$ and $k_2 = -6$, this difference becomes notable around 10^{-6}. Larger deviations of k_2 from -7 result in significant differences occurring at even higher failure probability levels. This behavior arises because changes in k_2 alter moments of the performance function, increasing the non-Gaussianity of the problem. MoM faces challenges to accurately evaluate small failure probabilities in cases of strong non-Gaussianity.

To sum up, the performance of the proposed method is largely influenced by the non-Gaussianility of the performance function, while both the statistical model and shape of the performance function will affect such non-Gaussianility. For weakly non-Gaussian problem, the proposed method can provide reliable failure probability estimation up to the level of 10^{-10}, while the accuracy of the proposed method will decrease for strongly non-Gaussian problem.

5.2. Example 2: Seepage problem below a dam modeled using finite element method

The second example involves the study of a steady state confined seepage below a dam as shown in Fig. 4, which is adopted from Ref. [43]. The failure event considered occurs when the seepage

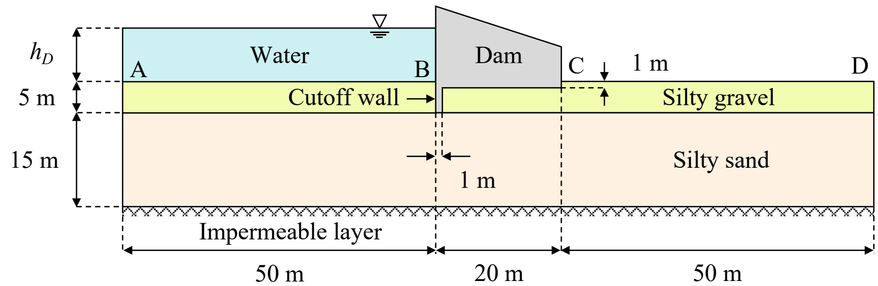

Figure 4: Schematic graph of the dam

discharge exceeds a prescribed threshold, and the corresponding performance function is constructed as follows:

$$G(\mathbf{X}) = b - Q(\mathbf{X}), \tag{33}$$

where b is the threshold, expressed in units of L/h/m; and $Q(\mathbf{X})$ is the seepage discharge, which is computed as follows:

$$Q(\mathbf{X}) = -\int_{\mathrm{CD}} k_{yy,2} \frac{\partial h_W}{\partial y} dx, \tag{34}$$

where CD represents the downstream side of the dam as shown in Fig 4; $k_{yy,2}$ is the vertical permeability of the second soil layer; and h_W is the hydraulic head, which is solved by the following differential equation:

$$k_{xx,i} \frac{\partial^2 h_W}{\partial x^2} + k_{yy,i} \frac{\partial^2 h_W}{\partial y^2} = 0, \quad i = 1, 2, \tag{35}$$

where $k_{xx,i}$ and $k_{yy,i}$ represent the horizontal and vertical permeabilities of the ith soil layer, respectively; and x and y denote horizontal and vertical coordinates, respectively. These permeabilities are considered as random variables, with the statistical information summarized in Table 1. The

Table 1: Statistical information of random variables in example 2

	Silty sand		Silty gravel	
	Horizontal $k_{xx,1}$ (m/s)	Vertical $k_{yy,1}$ (m/s)	Horizontal $k_{xx,2}$ (m/s)	Vertical $k_{yy,2}$ (m/s)
Distribution	Lognormal	Lognormal	Lognormal	Lognormal
Mean	5×10^{-7}	2×10^{-7}	5×10^{-6}	2×10^{-6}
Standard deviation	0.8×10^{-7}	0.4×10^{-7}	0.8×10^{-6}	0.4×10^{-6}

boundary conditions for Eq. (35) are as follows: (1) h_W over segments AB and CD are $20+h_D$ m and 20 m, respectively, where h_D=8.5 m is the height of water; (2) there is null flow across the other boundaries. To obtain sufficient accuracy, Eq. (35) is solved numerically applying a refined FEM as shown in Fig. 5a, where the associated model comprises 3413 nodes and 1628 quadratic triangular elements (details can be found in Ref [44]). This refined FEM is applied as the HF model. Using scripts implemented in MATLAB R2023b and executed on a computer with a 13th Gen Intel® Core™ i7-1360P processor running at 2.20 GHz, the computational time for the refined FEM is approximately 0.8301s.

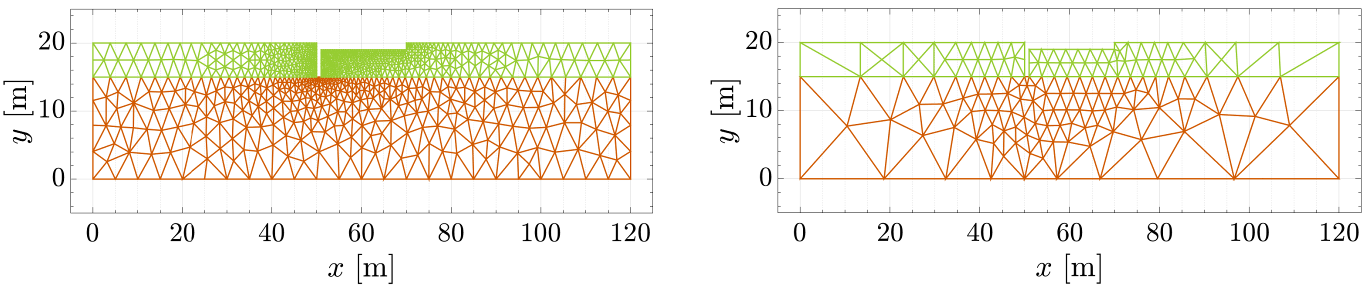

(a) High fidelity model

(b) Low fidelity model

Figure 5: FEMs of the dam

5.2.1. Moment estimation using different LF models

Based on Eq. (33), moments of the performance function can be easily obtained based on those of $Q(\mathbf{X})$ as follows:

$$\mu_{Z_1} = b - \mu_{Q_1}, \quad \mu_{Z_2} = \mu_{Q_2}, \quad \mu_{Z_3} = -\mu_{Q_3}, \quad \mu_{Z_4} = \mu_{Q_4}, \tag{36}$$

where μ_{Q_1}, μ_{Q_2}, μ_{Q_3} and μ_{Q_4} are the mean, standard deviation, skewness and kurtosis of $Q(\mathbf{X})$, respectively. Eq. (36) shows that, the key task for moment estimation of the performance function is to determine the moments of $Q(\mathbf{X})$. To compute these moments, an appropriate LF model needs to be constructed.

Since this is a linear problem, an efficient reduced-order model (ROM) can be constructed as the LF model (details can be found in Ref. [34]). This ROM consists of five basis terms and requires only 0.0017s per evaluation. However, as this ROM is applicable only to linear problems, a more general LF model is also developed by refining the finite element mesh, as illustrated in Fig. 5b. This coarse FEM consists of 268 elements and requires approximately 0.0189s per evaluation. The computational time ratios between these two LF models and the HF model are 488.3 and 43.9, respectively. The quality of the constructed LF models is evaluated by generating 3×10^4 samples of the seepage discharge, and the results are shown in Fig. 6. It is evident that the samples produced by the ROM exhibit a strong linear relationship with those from the refined FEM, whereas the relationship between the coarse and refined FEMs is weakly nonlinear.

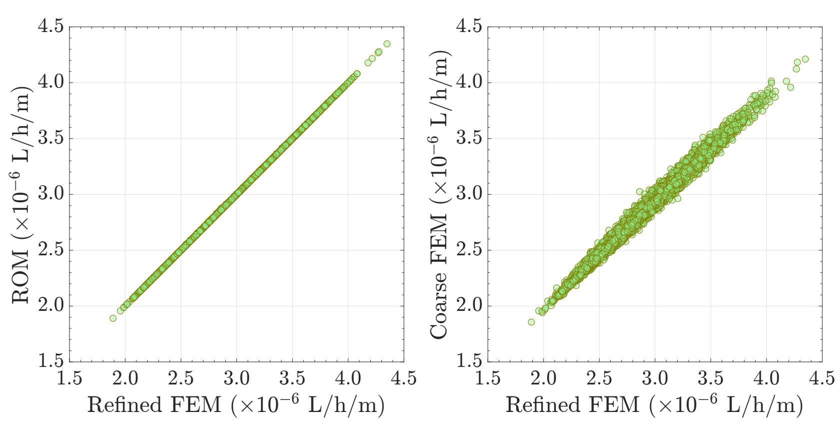

(a) Reduced order model (ROM)

(b) Coarse finite element model (FEM)

Figure 6: Samples of seepage discharge using different models

The moments of $Q(\mathbf{X})$ are estimated using the CV method based on these two LF models, with different sets of generated samples. For comparison, the moments are also computed using crude MCS with different sample sizes. Specifically, the MCS results based on 10^8 samples serve as the reference benchmark, while the results based on 6615 and 66150 samples are used for comparison with CV, combining ROM and coarse FEM, requiring the same computational time. The computed standard central moments of $Q(\mathbf{X})$, obtained from different methods, are compared in Table 2, alongside the CoVs of the raw moments, the number of model evaluations, and the corresponding computational time.

Table 2: Moments of the seepage discharge in example 2

	MCS			CV	
				ROM	Coarse FEM
N_H	10^8	6615	66150	6000	54000
N_L	0	0	0	3×10^5	3×10^5
T_t (s)	8.301×10^6	549.069	5050.14	549.06	5050.14
$\mu_{Q_1}(\times10^{-6})$	2.904	2.908	2.905	2.904	2.904
$\mu_{Q_2}(\times10^{-7})$	2.865	2.885	2.8701	2.863	2.860
μ_{Q_3}	0.281	0.2868	0.2901	0.281	0.280
μ_{Q_4}	3.141	3.2366	3.1613	3.139	3.155
CoV$[E_{Q_1}]$(%)	0.001	0.122	0.038	0.018	0.017
CoV$[E_{Q_2}]$(%)	0.015	1.839	0.5712	0.036	0.034
CoV$[E_{Q_3}]$(%)	0.101	12.80	3.884	0.054	0.052
CoV$[E_{Q_4}]$(%)	0.039	4.875	1.518	0.074	0.071

μ_{Q_1} and μ_{Q_2} have unit of L/h/m.
N_H denotes the number of HF model evaluations required.
N_L denotes the number of LF model evaluations required.
T_t denotes the total computational time required.

As shown in Table 2, the moments of $Q(\mathbf{X})$ estimated using CV achieve CoVs comparable to those obtained from MCS with 10^8 samples, but with significantly reduced computational time. This efficiency is due to the fact that CV leverages LF models to reduce the variance of the estimators, requiring far fewer HF model evaluations compared to MCS. Furthermore, for the same computational time, the CoVs of the moments obtained using CV are less than 1/20 of those from MCS. When comparing CV with coarse FEM to CV with ROM, the latter achieves acceptable CoVs for moments with even fewer HF model evaluations. This is due to the strong linear relationship between the ROM and the HF model, which facilitates further reduction in the variance of moments. Such a difference highlights the critical role of enhancing the linear relationship between HF and LF models to improve the performance of the proposed method.

5.2.2. Failure probability and convergence rate

With the moments of $Q(\mathbf{X})$ obtained, moments of $G(\mathbf{X})$ with different values of b can be readily obtained based on Eq. (36). Then, MoM can be applied to compute the corresponding failure probabilities, which are depicted in Fig. 7. For comparison, the failure probability is also computed using MoM based on different samples from HF models and crude MCS with 10^8 samples, and the results are also depicted in Fig. 7.

It can be found from Fig. 7 that, for all the thresholds considered, the proposed method can obtain nearly the same results as those from crude MCS when considering $N_H = 10^8$ samples, which demonstrates the accuracy of the proposed method for this example. The results obtained from MoM with $N_H = 6615$ and $N_H = 66150$ have relatively significant difference from those of the MCS when $N_H = 10^8$, which is attributed to the error in the estimated moments.

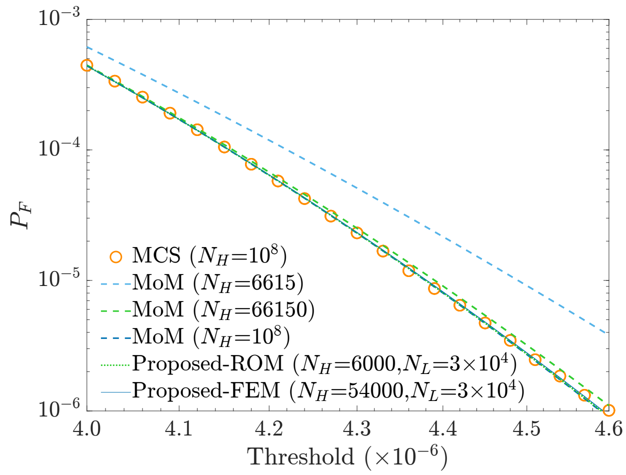

Figure 7: Failure probability for example 2

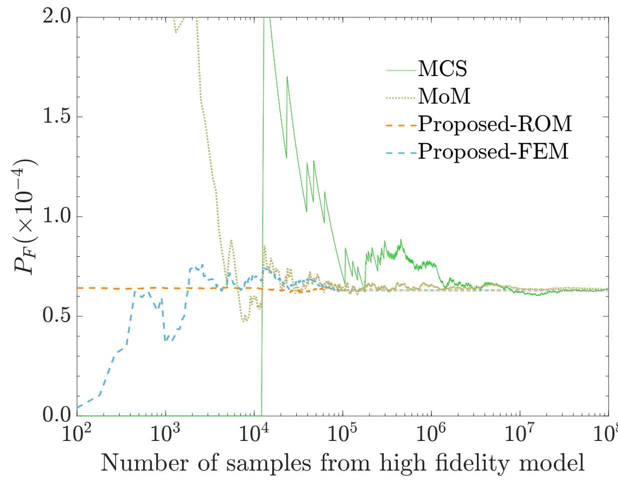

Figure 8: Failure probability with different number of samples in example 2

To assess the convergence speed of the proposed method, the failure probabilities obtained from both MCS, MoM with moments estimated from MCS and the proposed method are compared in Fig. 8 for the case where b=4.2 $\times10^{-6}$ L/h/m. The total sample size applied for the proposed method is 10^5, with auxiliary lines included in the figure for better clarity. It is important to note that although the proposed method requires additional samples from the LF model compared to crude MCS, the computational time for these extra samples is relatively small. As shown in Fig. 8, the results obtained by the proposed method based on ROM converge after 1,000 samples, while those based on coarse FEM converge after around 7×10^4 samples. Both methods based on the proposed approach converge much earlier than crude MCS. Meanwhile, the results obtained from MoM based on moments estimated from MCS converge after around 10^6, which is almost the same as crude MCS. This demonstrates the efficiency of the proposed method for this example.

5.3. Example 3: Nonlinear Duffing oscillator with high dimensional inputs

In this example, a nonlinear Duffing oscillator with a single degree of freedom is considered. This type of oscillator is commonly used to model systems exhibiting cubic stiffness nonlinearity. The objective is to estimate the system's first excursion probability. The corresponding performance function is defined as follows:

$$G(\mathbf{X}) = b - \max\{t \in [0,\ T] : |y(\mathbf{X},t)|\}, \tag{37}$$

where b is the threshold expressed in m; t is time instants in s; $T = 15$s is the time duration considered; and $y(\mathbf{X},t)$ is the displacement of the system, which is computed by the governing equation of motion as follows:

$$m\ddot{y}(\mathbf{X},t) + c\dot{y}(\mathbf{X},t) + ky(\mathbf{X},t) + k_3y^3(\mathbf{X},t) = p(\mathbf{X},t), \tag{38}$$

where $m = 6 \times 10^4$kg is the mass; $c = 2\zeta\sqrt{km}\,$N s/m is the damping coefficient; $\zeta = 0.05$ is the damping ratio; $k = 5 \times 10^6\,$N/m is the linear stiffness; $k_3 = 1 \times 10^6$ N/m^3 is the cubic stiffness; $p(\mathbf{X},t)$ represents an external excitation in the unit of N; $\dot{y}(\mathbf{X},t)$ is the velocity; and $\ddot{y}(\mathbf{X},t)$ is the acceleration. The system starts from rest, with $y(\mathbf{X},0) = 0$m and $\dot{y}(\mathbf{X},0) = 0$m/s.

The external force $p(\mathbf{X}, t)$ is defined as:

$$p(\mathbf{X}, t) = -m \sum_{i=1}^{n} \sqrt{4S\Delta\omega} \cos(\omega_i t + X_i), \tag{39}$$

where $n = 150$ is the dimension of $\mathbf{X}$; $S = 0.03\,\mathrm{m}^2/\mathrm{s}^3$ is the intensity of the white noise power spectral density; $\Delta\omega = \omega_{\max}/n$ is the frequency increment; $\omega_{\max} = 30$ rad/s is the maximum frequency; $\omega_i = \omega_{\min} + (i-1)\Delta\omega$, with $\omega_{\min} = \Delta\omega$; and X_i is the ith component of $\mathbf{X}$, which follows a uniform distribution in $[0, 2\pi]$. To ensure the accuracy of the simulation, a time step of $\Delta t_{\mathrm{HF}} = 0.015\,\mathrm{s}$ is used, resulting in $n_{\mathrm{t,HF}} = 1001$ time instants, with the corresponding time vector $t_j^{\mathrm{HF}} = (j-1)\Delta t_{\mathrm{HF}}$ for $j = 1, 2, \ldots, n_{\mathrm{t,HF}}$.

To conduct the proposed method for reliability analysis, a LF model is constructed with a coarser time step of $\Delta t_{\mathrm{LF}} = 0.12\,\mathrm{s}$, producing $n_{\mathrm{t,LF}} = 126$ time instants, with the corresponding time vector $t_j^{\mathrm{LF}} = (j-1)\Delta t_{\mathrm{LF}}$ for $j = 1, 2, \ldots, n_{\mathrm{t,LF}}$. The ratio of computational time between the HF and LF model evaluations is around 44.06. For CV, the sample sizes n and m are set to be 2400 and 9×10^4, respectively. The first four raw moments of extreme response within the total simulation time T and corresponding CoVs can be obtained as (0.0917m, $8.6471 \times 10^{-3}\mathrm{m}^2$, $8.3919 \times 10^{-4}\mathrm{m}^3$ $8.3726 \times 10^{-5}\mathrm{m}^4$) and (0.1074%, 0.2213%, 0.3494%, 0.4994%), respectively. Based on the raw moments, the mean, standard variation, skewness and kurtosis of the extreme response are obtained as 0.0917m, 0.0157m, 0.3832, and 3.1894, respectively. For comparison, the crude MCS based on HF model is also conducted. To obtain raw moments with similar level of CoVs as CV, the samples required by crude MCS is around 2.2×10^4. The ratio of computational time between crude MCS and CV for moment estimation is approximately 4.95. Furthermore, MoM based on moments estimated using MCS with samples from HF model is also conducted. To obtain same computational time between MoM and the proposed method, the sample size of HF model applied in MoM is 4445. The mean, standard variation, skewness and kurtosis of the extreme response from crude MCS are obtained as 0.0919m, 0.0155m, 0.3441, and 3.0883, respectively. The CoVs of first raw moments are (0.25%, 0.51%, 0.78%, 1.07%). Comparison between the moment estimations conducted from crude MCS and CV shows that the application of CV can significantly reduce the variance of moments.

Based on moments of extreme value of response, moments of $G(\mathbf{X})$ can be easily computed and the corresponding failure probability can be readily obtained. For comparison, failure probability is also estimated using crude MCS with 10^8 samples evaluated using the HF model, MoM with 4445 samples evaluated usign the HF model, and the variations of the failure probability with the threshold b is shown in Fig. 9.

It can be observed that the failure probability estimated by the proposed method aligns well with that obtained from MCS for $P_F \geq 10^{-4}$, demonstrating the accuracy of the proposed method for nonlinear and high-dimensional problems. In contrast, the failure probability estimated using MoM shows a relatively significant deviation from the MCS results, primarily due to inaccuracies in moment estimation. For failure probabilities smaller than 10^{-4}, a noticeable discrepancy arises between the results of the proposed method and those from MCS. This is because the first four standard central moments of $G(\mathbf{X})$ are insufficient to accurately characterize the tail behavior of the probability density function (PDF).

Furthermore, to assess the convergence speed of the proposed method, Fig. 10 illustrates the variations in failure probability as a function of the number of HF samples used by the proposed method, MoM, and MCS. It can be seen that the proposed method converges significantly faster than MoM, and its convergence rate is influenced by the failure probability. When the failure probability is relatively large (around 10^{-4} for $b = 0.16$ m), the proposed method yields reliable results with

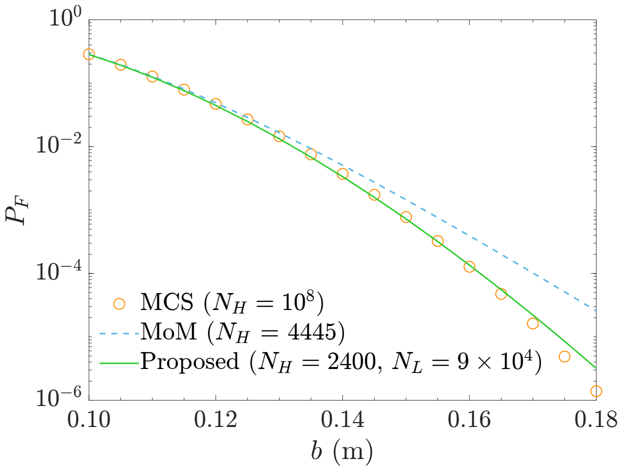

Figure 9: Failure probability for different thresholds in example 3

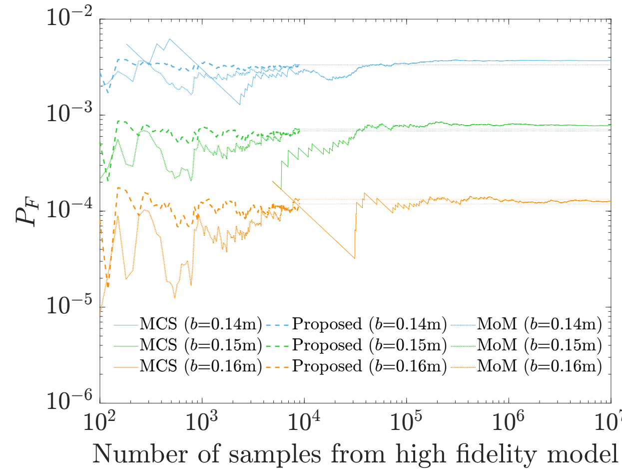

Figure 10: Failure probability with different number of samples in example 3

approximately 1000 HF samples.

6. Discussion and Conclusions

A novel reliability analysis method is proposed, combining Method of Moments (MoM) and Control Variates (CV). Unbiased estimators for the third and fourth raw moments of the performance function have been developed using CV, along with their variances. Three examples are investigated, including non-Gaussian polynomial, complex FEMs, and nonlinear dynamic systems.

The key feature of the proposed method lies in the integration of MoM and CV, with accuracy and efficiency determined by MoM and CV, respectively. Specifically, accuracy is influenced by the non-Gaussianity of the performance function. For weakly non-Gaussian problems, where the skewness and kurtosis of the performance function are close to 0 and 3, respectively, the proposed method can achieve accurate estimations of small failure probabilities (down to 10^{-10}). The computational efficiency is independent of the dimensionality of the input random variables and is primarily influenced by the quality of the low-fidelity model used in CV.

While the proposed method offers significant advantages in terms of accuracy and computational efficiency, certain considerations should be noted to ensure its optimal application. The method leverages a moment-based reliability index, which performs effectively when the first four moments adequately characterize the distribution of the performance function. However, in scenarios involving multi-modal behaviors or strongly non-Gaussian distributions, the accuracy may be affected. In terms of efficiency, the proposed method benefits from the use of low-fidelity models, which must maintain a strong linear correlation with the high-fidelity counterparts. This correlation is best achieved when both models share the same underlying physical mechanisms. Practical approaches, such as modifying element size in finite element models or adjusting time steps in dynamic load simulations, have proven to be effective. Nonetheless, for highly complex systems, maintaining both efficiency and correlation can be challenging. These cases provide a valuable direction for further investigation into more flexible model reduction strategies to enhance the scalability of the approach.

Acknowledgment

The study is partially supported by the Alexander von Humboldt Foundation for the postdoctoral grant of Xuan-Yi Zhang and the Henriette Herz Scouting program (Matthias G.R. Faes). The research is also funded by the Deutsche Forschungsgemeinschaft (DFG, German Research Foundation) under project number 527637016. The authors gratefully acknowledge the supports.

Appendix A. Complete expressions of fourth moment reliability index

Complete monotonic expressions of fourth moment reliability index $\beta_{4\mathrm{M}}$[37, 38] are shown in Table A.1. The parameters required are computed as follows:

$$J_1 = 2a_1a_4(|p|^{3/2} - q) + \beta_{2\mathrm{M}}, \quad J_2 = 2a_1a_4(-|p|^{3/2} - q) + \beta_{2\mathrm{M}}, \tag{A.1}$$

$$J_0 = a_2^2/4a_3 + a_3, \quad \phi = \arccos\left(-\frac{q}{|p|^{3/2}}\right), \tag{A.2}$$

$$\beta_0 = \frac{a_2 - \sqrt{a_2^2 + 4a_3(a_3 - \beta_{2M}/a_1)}}{2a_3}, \tag{A.3}$$

$$\beta_1 = \sqrt[3]{\Delta + q} - \sqrt[3]{\Delta - q} + \frac{a_3}{3a_4}, \tag{A.4}$$

$$\beta_2 = 2\mathrm{cos}\left(\frac{\phi + \pi}{3}\right)\sqrt{-p} + \frac{a_3}{3a_4}, \quad \beta_3 = -2\mathrm{cos}\left(\frac{\phi}{3}\right)\sqrt{-p} + \frac{a_3}{3a_4}, \tag{A.5}$$

$$\beta_4 = 2\mathrm{cos}\left(\frac{\phi - \pi}{3}\right)\sqrt{-p} + \frac{a_3}{3a_4}. \tag{A.6}$$

Table A.1: Complete monotonic expressions of fourth moment reliability index β_{4M}

μ_{Z_4}	p	μ_{Z_3}	β_{2M}	β_{4M}
$[5/3 + 4\mu_{Z_3}^2/3,\ 3 + 4\mu_{Z_3}^2/3]$	$(-\infty, 0]$	$(-\infty, +\infty)$	$[J_1, J_2]$	β_2
$3 + 4\mu_{Z_3}^2/3$	NA	$(-\infty, 0]$	$[J_0, +\infty)$	β_0
		$[0, +\infty)$	$(-\infty, J_0]$	β_0
$(3 + 4\mu_{Z_3}^2/3, 48)$	$[0, +\infty)$	$(-\infty, +\infty)$	$(-\infty, +\infty)$	β_1
	$(-\infty, 0)$	$[0, +\infty)$	$(-\infty, J_1]$	β_3
		$(-\infty, 0)$	$[J_2, +\infty)$	β_4

NA denotes not available.

Appendix B. Raw moments of an univariate polynomial and the failure probability

Consider a polynomial of a single random variable X defined in Eq. (31). The ith raw moment, i.e., E_{Z_i}, can be computed as follows:

$$E_{Z_i} = \mathbb{E}[(G(X))^i] = \mathbb{E}[(k_1X^3 + k_2X^2 + k_3X + k_4)^i], \tag{B.1}$$

Expanding Eq. (B.1), the first four raw moments of $Z = G(X)$ are given as follows:

$$E_{Z_i} = \sum_{q+j+l+m=i} \binom{i}{q, j, l, m} k_1^q k_2^j k_3^l k_4^m E_{X_{3q+2j+l}}, \tag{B.2}$$

where $E_{X_{3q+2j+l}}$ is the $(3q + 2j + l)$th raw moment of X.

The failure probability is defined as the probability of $G(X) \leq 0$. As $G(X)$ is a univariate polynomial, the roots of $G(X) = 0$ can be analytically obtained using the Cardano formula. The corresponding failure probability is then computed as:

$$k_1 > 0: \quad P_F = F_X(x_1) + F_X(x_3) - F_X(x_2), \tag{B.3}$$

$$k_1 < 0: \quad P_F = 1 - [F_X(x_1) + F_X(x_3) - F_X(x_2)], \tag{B.4}$$

where $F_X(\cdot)$ is the CDF of X; and $x_1 \leq x_2 \leq x_3$ are the roots of $G(X) = 0$.

References

[1] T. C. Hesterberg, B. L. Nelson, Control variates for probability and quantile estimation, Management Science 44 (9) (1998) 1295–1312.

[2] Z. Wang, Optimized equivalent linearization for random vibration, Structural Safety 106 (2024) 102402.

[3] R. Melchers, Importance sampling in structural systems, Structural safety 6 (1) (1989) 3–10.

[4] B. Peherstorfer, K. Willcox, M. Gunzburger, Survey of multifidelity methods in uncertainty propagation, inference, and optimization, Siam Review 60 (3) (2018) 550–591.

[5] O. Ditlevsen, P. Bjerager, R. Olesen, A. Hasofer, Directional simulation in gaussian processes, Probabilistic Engineering Mechanics 3 (4) (1988) 207–217.

[6] M. A. Misraji, M. A. Valdebenito, H. A. Jensen, C. F. Mayorga, Application of directional importance sampling for estimation of first excursion probabilities of linear structural systems subject to stochastic gaussian loading, Mechanical Systems and Signal Processing 139 (2020) 106621.

[7] S.-K. Au, J. L. Beck, Estimation of small failure probabilities in high dimensions by subset simulation, Probabilistic engineering mechanics 16 (4) (2001) 263–277.

[8] L. S. Katafygiotis, S. Cheung, Application of spherical subset simulation method and auxiliary domain method on a benchmark reliability study, Structural Safety 29 (3) (2007) 194–207.

[9] O. Ditlevsen, H. O. Madsen, Structural reliability methods, Vol. 178, Wiley New York, 1996.

[10] Y. G. Zhao, T. Ono, A general procedure for first/second-order reliabilitymethod (FORM/SORM), Structural safety 21 (2) (1999) 95–112.

[11] K. Breitung, FORM/SORM, SS and MCMC: A mathematical analysis of methods for calculating failure probabilities, in: International Probabilistic Workshop, Springer, 2021, pp. 353–367.

[12] L. S. Katafygiotis, K. M. Zuev, Geometric insight into the challenges of solving high-dimensional reliability problems, Probabilistic Engineering Mechanics 23 (2-3) (2008) 208–218.

[13] I. Kaymaz, Application of kriging method to structural reliability problems, Structural safety 27 (2) (2005) 133–151.

[14] V. Dubourg, B. Sudret, J.-M. Bourinet, Reliability-based design optimization using kriging surrogates and subset simulation, Structural and Multidisciplinary Optimization 44 (2011) 673–690.

[15] D.-W. Jia, Z.-Y. Wu, An importance sampling reliability method combining kriging and gaussian mixture model through ring subregion strategy for multiple failure modes, Structural and Multidisciplinary Optimization 65 (2) (2022) 61.

[16] G. Blatman, B. Sudret, Adaptive sparse polynomial chaos expansion based on least angle regression, Journal of computational Physics 230 (6) (2011) 2345–2367.

[17] N. L"uthen, S. Marelli, B. Sudret, Sparse polynomial chaos expansions: Literature survey and benchmark, SIAM/ASA Journal on Uncertainty Quantification 9 (2) (2021) 593–649.

[18] X. Han, C. Jiang, L. Liu, J. Liu, X. Long, Response-surface-based structural reliability analysis with random and interval mixed uncertainties, Science China Technological Sciences 57 (2014) 1322–1334.

[19] X. Huang, Y. Liu, Y. Zhang, X. Zhang, Reliability analysis of structures using stochastic response surface method and saddlepoint approximation, Structural and Multidisciplinary Optimization 55 (2017) 2003–2012.

[20] C. Dang, A. Cicirello, M. A. Valdebenito, M. G. Faes, P. Wei, M. Beer, Structural reliability analysis with extremely small failure probabilities: A quasi-Bayesian active learning method, Probabilistic Engineering Mechanics 76 (2024) 103613.

[21] C. Dang, T. Zhou, M. A. Valdebenito, M. G. Faes, Yet another Bayesian active learning reliability analysis method, Structural Safety 112 (2025) 102539.

[22] M. A. Bouhlel, J. R. Martins, Gradient-enhanced kriging for high-dimensional problems, Engineering with Computers 35 (1) (2019) 157–173.

[23] J. Li, J. Chen, Stochastic dynamics of structures, John Wiley & Sons, 2009.

[24] D. Yang, G. Chen, Stochastic dynamic analysis of large-scale nonlinear structures, in: Advances in Applied Nonlinear Dynamics, Vibration and Control-2021: The proceedings of 2021 International Conference on Applied Nonlinear Dynamics, Vibration and Control (ICANDVC2021) 1, Springer, 2022, pp. 845–859.

[25] C. Dang, M. Beer, Semi-Bayesian active learning quadrature for estimating extremely low failure probabilities, Reliability Engineering & System Safety 246 (2024) 110052.

[26] T. Zhou, Y. Peng, J. Li, An efficient reliability method combining adaptive global metamodel and probability density evolution method, Mechanical Systems and Signal Processing 131 (2019) 592–616.

[27] Y. G. Zhao, T. Ono, Moment methods for structural reliability, Structural safety 23 (1) (2001) 47–75.

[28] Y. G. Zhao, Z. H. Lu, Structural reliability: approaches from perspectives of statistical moments, John Wiley & Sons, 2021.

[29] H. Xu, S. Rahman, A generalized dimension-reduction method for multidimensional integration in stochastic mechanics, International Journal for Numerical Methods in Engineering 61 (12) (2004) 1992–2019.

[30] J. Xu, C. Dang, A new bivariate dimension reduction method for efficient structural reliability analysis, Mechanical Systems and Signal Processing 115 (2019) 281–300.

[31] M. B. Giles, Multilevel monte carlo path simulation, Operations research 56 (3) (2008) 607–617.

[32] B. Peherstorfer, K. Willcox, M. Gunzburger, Optimal model management for multifidelity monte carlo estimation, SIAM Journal on Scientific Computing 38 (5) (2016) A3163–A3194.

[33] S. S. Lavenberg, T. L. Moeller, P. D. Welch, Statistical results on control variables with application to queueing network simulation, Operations Research 30 (1) (1982) 182–202.

[34] I. González, M. A. Valdebenito, J. Correa, H. A. Jensen, Calculation of second order statistics of uncertain linear systems applying reduced order models, Reliability Engineering & System Safety 190 (2019) 106514.

[35] C. H. Acevedo, M. A. Valdebenito, I. V. González, H. A. Jensen, M. G. Faes, Y. Liu, Control variates with splitting for aggregating results of monte carlo simulation and perturbation analysis, Structural Safety 108 (2024) 102445.

[36] Y. G. Zhao, X. Y. Zhang, Z. H. Lu, A flexible distribution and its application in reliability engineering, Reliability Engineering & System Safety 176 (2018) 1–12.

[37] Y. G. Zhao, X. Y. Zhang, Z. H. Lu, Complete monotonic expression of the fourth-moment normal transformation for structural reliability, Computers & Structures 196 (2018) 186–199.

[38] X. Y. Zhang, Y. G. Zhao, Z. H. Lu, Unified hermite polynomial model and its application in estimating non-gaussian processes, Journal of Engineering Mechanics 145 (3) (2019) 04019001.

[39] T. Wang, D.-G. Lu, Y.-Q. Tan, Refined dimension-reduction integration method for uncertainty propagation in stochastic systems: estimation of statistical moments, Reliability Engineering & System Safety (2024) 110753.

[40] G. Fishman, Monte Carlo: concepts, algorithms, and applications, Springer Science & Business Media, 2013.

[41] A. N. Avramidis, J. R. Wilson, A splitting scheme for control variates, Operations Research Letters 14 (4) (1993) 187–198.

[42] S.-K. Au, J. L. Beck, Important sampling in high dimensions, Structural safety 25 (2) (2003) 139–163.

[43] M. A. Valdebenito, H. A. Jensen, H. Hernández, L. Mehrez, Sensitivity estimation of failure probability applying line sampling, Reliability Engineering & System Safety 171 (2018) 99–111.

[44] K. J. Bathe, Finite element procedures, Prentice Hall, 2006.